A Hybrid Barometric/Ultrasonic Altimeter for Aiding ZUPT-based Inertial Pedestrian Navigation Systems

Chi-Shih Jao, Yusheng Wang, Yu-Wei Lin, and Andrei M. Shkel
MicroSystems Lab, University of California, Irvine

BIOGRAPHYIES

Chi-Shih Jao is a Ph.D. student in the Department of Mechanical and Aerospace Engineering at the University of California, Irvine, CA, USA, and a member of the MicroSystems Laboratory. He received a B.S. in Electrical Engineering from National Tsing Hua University (NTHU), Hsinchu, Taiwan, in 2015, and a M.S. in Electrical Engineering from the Pennsylvania State University, State College, PA, USA, in 2018. In 2019, he received Paul and Beverly Holmes Endowed Fellowships. His research interests are in inertial navigation, indoor navigation, Micro-Electro-Mechanical System (MEMS), and computer vision.

Yusheng Wang received the B.Eng. degree (Hons.) in engineering mechanics from Tsinghua University, Beijing, China, in 2014, and the Ph.D. degree in mechanical and aerospace engineering from the University of California, Irvine, CA, USA, in 2020. His research interests include design, analysis, fabrication, post-processing, and characterization of 3-D micro-machined resonators, and pedestrian inertial navigation development. He is a recipient of the 2016-2017 Paul and Beverly Holmes Fellowship, the Student Paper Award at IEEE Inertial 2019, and the best post-graduate presentation award at 22nd Conference of Young Scientists — Navigation and Motion Control.

Yu-Wei Lin received the B.S. degree in engineering mechanics from University of Illinois at Urbana Champaign, IL, USA, in 2014, and the M.S. degree in mechanical engineering from University of California Irvine, CA, USA, in 2016. He is currently pursuing the Ph.D. degree in mechanical engineering in University of California Irvine. His research interests include design, fabrication, and control of vibratory inertial sensors and capacitive micromachined ultrasonic transducers (CMUT).

Andrei M. Shkel received the Diploma (Hons.) degree in mechanics and mathematics from Lomonosov Moscow State University, Moscow, Russia, in 1991, and the Ph.D. degree in mechanical engineering from the University of Wisconsin, Madison, WI, USA, in 1997. In 2000, he joined the Faculty of the University of California at Irvine (UCI), Irvine, CA, USA, where he is currently a Professor with the Department of Mechanical and Aerospace Engineering, with joint appointments with the Department of Electrical Engineering and Computer Science and the Department of Biomedical Engineering. He served as a Program Manager of Microsystems Technology Office, Defense Advanced Research Projects Agency, Arlington, VA, USA, from 2009 to 2013. His research interests, reflected in more than 250 peer-reviewed publications and two books, include solid-state sensors and actuators, microelectromechanical-system-based neuroprosthetics, sensor-based intelligence, and control theory. He holds 41 U.S. patents. Dr. Shkel was a recipient of the 2002 George E. Brown, Jr., Award, the 2005 National Science Foundation CAREER Award, the 2006 UCI HSSoE Best Faculty Research Award, the 2009 IEEE Sensors Council Technical Achievement Award, and the 2020 UCI HSSoE Innovator of the Year Award. In 2013, he received the Office of the Secretary of the Defense Medal for Exceptional Public Service. He served as the Founding Chair of the IEEE International Symposium on Inertial Sensors and Systems. He has served on a number of Editorial Boards, most recently, as Subject Editor for the IEEE JOURNAL OF MICROELECTROMECHANICAL SYSTEMs and Board Member of JOURNAL OF GYROSCOPY AND NAVIGATION. He currently serves as the President of the IEEE Sensors Council (2020-2021) and a member of the IEEE Technical Advisory Board (TAB). Dr. Shkel is the Fellow of IEEE.

ABSTRACT

In this paper, we propose a hybrid altimeter for foot-mounted Inertial Navigation Systems (INS) aided by a barometer and a downward-facing ultrasonic sensor. The goal of developing the hybrid altimeter was to minimize the usage of barometric altimeter in height estimation as measurements of barometers are affected by changes in ambient temperature and air pressure. In this paper, we show that a shoe-mounted downward-facing ultrasonic sensor alone could be used as an altimeter on a variety of terrains, from

 https://doi.org/10.33012/2020.17699

flat surfaces to uneven stairs, by simultaneously estimating shoe height and floor elevation. We will refer to this type of altimeter as the ultrasonic altimeter. To account for other common indoor terrains, such as ramps and elevators, the developed hybrid altimeter uses a Multi-Model Kalman Filter to fuse measurements of a barometer and the ultrasonic altimeter. In the fusion process, the hybrid altimeter adaptively selects weights for the barometric and ultrasonic measurements based on the terrains under operation. We utilized a foot-mounted Inertial Measurement Unit (IMU) to realize the detection of elevators and ramps. We conducted three series of experiments to test the performance of the proposed hybrid altimeter. The first experiment showed that the proposed altimeter is less sensitive to temperature and air pressure changes in the surrounding environment than a barometer. The second series of experiments investigated the performance of the hybrid altimeter in the case of walking slowly on a flat plane, and the corresponding experimental results indicated that the Zero velocity UPdaTe (ZUPT)-based INS aided by the hybrid altimeter improved the Root Mean Square Error (RMSE) along the vertical direction by 96%, as compared to the standalone ZUPT-based INS, and by 97%, when compared to the ZUPT-based INS aided by the barometer. In the third series of experiments, we studied the navigation accuracy of the hybrid altimeter for common indoor terrains, such as flat surfaces, stairs, ramps, and elevators. The results of this series of experiments showed that the RMSE of the ZUPT-based INS aided by the hybrid altimeter outperformed the RMSE of the standalone ZUPT-based INS by 91%. When compared to the RMSE of the ZUPT-based INS aided by the barometer vs. the hybrid altimeter, in the latter case the accuracy was increased by 41% ($0.15\ m$). The primary residual error sources, in our opinion, contributing to the vertical errors of the ZUPT-based INS aided by the hybrid altimeter are the underestimate of stair height and the false alarm of stair detection of the ultrasonic altimeter.

I. INTRODUCTION

Developing an accurate indoor navigation system is essential for first responders, firefighters, and rescuers, who often conduct missions in Global Navigation Satellite System (GNSS)-challenged environments. In such environments, the positioning may also be carried out with radio navigation systems using signals from Wireless Local Area Networks (WLAN), Bluetooth, or Long-Term Evolution (LTE) [1, 2, 3]. However, in some scenarios, the assumption about availability of Radio-Frequency (RF) infrastructure might not be realistic. Pedestrian Dead Reckoning (PDR), or self-contained pedestrian Inertial Navigation Systems (INS) are the only remaining options in such RF-challenged environments.

The successful development of Micro-Electro-Mechanical System (MEMS) technology has enabled pedestrian INS to use small-size low-cost Inertial Measurement Units (IMUs). However, navigation solutions, when based solely on dead reckoning IMU measurements, have high drift in estimation of positions. For pedestrian navigation, Zero velocity UpdaTe (ZUPT) is a method that has been widely applied to assist INS by zeroing out the residual velocity, generated by the varying biases of IMUs, during the stance phases, allowing to effectively constrain error growth in velocity estimations without increasing the system complexity [4, 5, 6, 7]. With a proper setting of the ZUPT threshold and compensation for its systematic errors, the ZUPT-aided INS is capable of achieving an accuracy of 1 meter after traveling on the order of 100 meters, with industrial-grade inertial sensors [8, 9].

For first responders, the precision of height estimation is a crucial performance metrics. For example, an accumulated three-meters of error in the vertical direction is equivalent to an error in identification of the floor in a building [10]. The navigation errors coming from the ZUPT-based INS accumulate unboundly in the vertical direction [11]. Thus, additional sensing modalities can be effectively used along with the ZUPT-based INS to enhance the navigation accuracy, in-plane and out-of-plane. Barometric altimeters (barometers) are popular devices for this purpose as they provide independent and direct measurements of position along the vertical direction. Barometric data for INS has been shown to improve the overall navigation results in various types of integrated INS [12, 13, 14, 15, 16, 17, 18]. However, because these devices detect changes in air pressure, their measurements are easily affected by weather changes during data acquisition, elevated pressure due to temperature increase in the event of fire, and other environmental effects [19]. Although this issue can be addressed by using one or multiple reference barometers at known locations [20, 21, 22, 23, 24], this type of solution is not suitable for infrastructure-free navigation. Moreover, barometers are easily subjected to air pressure perturbations in local environments. For example, opening a door or a window near the sensor would lead to incorrect estimation of height [21], and those errors could be further amplified in chaotic air pressure environments [25, 26].

An alternative sensor that can be employed to obtain information about the relative vertical position is an ultrasonic sensor [27, 28, 29, 10]. A downward-facing ultrasonic sensors can measure the distance between the sensor and the ground. In [10], for example, an ultrasonic sensor was mounted on the bottom of a backpack to detect a relative height distance. This information was fused with height measurements collected from a barometer and used in the Kalman Filter framework. Such arrangement has been demonstrated to handle effectively the pressure shock during navigation and allowed to estimate the barometer bias during the transition between indoor and outdoor environments. However, the Kalman filter discussed in [10] depends highly on barometric measurements, and

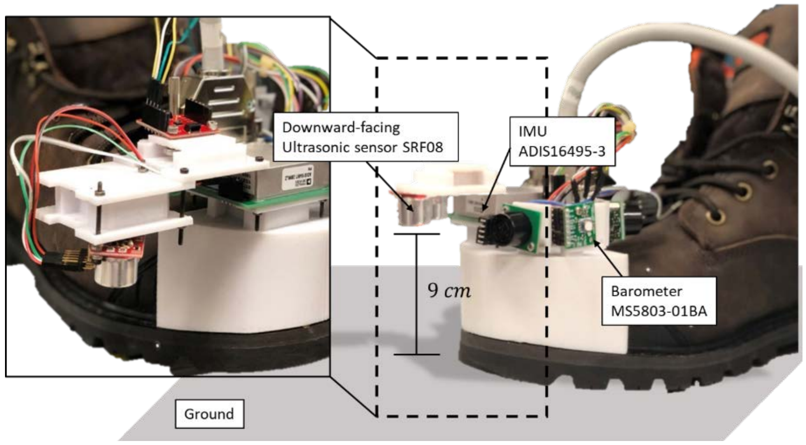

Fig. 1. The Lab-On-Shoe platform integrated with a downward-facing ultrasonic sensor SRF08 and a barometric altimeter MS5803-01BA.

those can be inaccurate due to, for example, the room temperature controlled by air-conditioning or other chaotic variations under extreme operational cases. In pedestrian navigation, rich information can be extracted from the dynamics of a human walk. The mechanism introduced in [10], if used to aid ZUPT-based INS, can provide a bound for displacement error growth in the vertical direction, but cannot capture subtle foot motions, which could benefit the overall navigation results of a pedestrian INS. In [30], downward-facing ultrasonic sensors were mounted on the shoe to extract measurements of the height of a shoe relative the ground. Although the method showed an improvement of navigation accuracy in experiments of walking on a flat surface, as compared to standalone ZUPT-aided INS, it did not account for other common indoor terrains, such as stairs, ramps, and elevators.

In this paper, we propose a hybrid altimeter that uses a shoe-mounted ultrasonic altimeter and a shoe-mounted barometer for aiding ZUPT-based INS. One of the goals of this approach is to minimize the usage of barometers during indoor navigation. The shoe-mounted ultrasonic sensor was placed on a toe side of pedestrian's shoe, facing downward to the ground. The measurement is the height of the shoe relative to the ground. We use the Kalman filter to convert ultrasonic readouts to altitude data relative to the initial location and refer to this type of altimeter as the ultrasonic altimeter. To extend the usage of the ultrasonic altimeter, we developed a hybrid framework that fuses a barometer and an ultrasonic altimeter. In the fusion process, the ultrasonic altimeter receives more weights when the hybrid system detects that the pedestrian is walking on a flat plane or stairs. For the case of slopes or inside elevators, the hybrid system would prioritize the barometer measurements. The detection of flat planes, slopes, and elevators would be achieved with information obtained instantaneously from an IMU. This configuration not only limits the error growth of an INS in the vertical direction but also enables capturing the foot motions, which is subsequently used to aid ZUPT-augmented INS. This paper makes the following contributions:

1) it allows a shoe-mounted ultrasonic sensor to be used as an altimeter in the case of walking on flat plane or stairs,
2) it introduces for the first time a hybrid altimeter that uses both the ultrasonic altimeter and the barometer,
3) it presents an Extended Kalman Filter (EKF) to fuse the hybrid altimeter measurements with a ZUPT-augmented Inertial Navigation System,
4) it verifies the proposed method with in-field experiments.

This paper is organized as follows. In Section II, the configuration of using ultrasonic sensors as an aiding altimeter for the cases of flat planes and stairs, and the corresponding Kalman Filter configuration is discussed. In Section III, we demonstrate a framework for the hybrid approach for integrating the ultrasonic sensor and the barometer. We also discuss the elevator detection and ramp detection using an IMU in Section III. In Section IV, we evaluate the navigation performance of ZUPT-based INS aided by the hybrid ultrasonic/barometric altimeter with indoor walking experiments. Finally, Section V concludes the paper.

II. ULTRASONIC ALTIMETER

A shoe-mounted downward-facing ultrasonic sensor is capable of finding relative distances between the shoe and the ground. To use the sensor as an altimeter, we convert the relative distance to the height of the shoe in the navigation frame by simultaneously estimating the vertical position of the floor in the navigation frame. In the case of walking on flat surfaces and stairs, the estimation of floors can be achieved based on two phenomena: 1) ultrasonic measurements are smooth in the case of flat surfaces, and 2) a

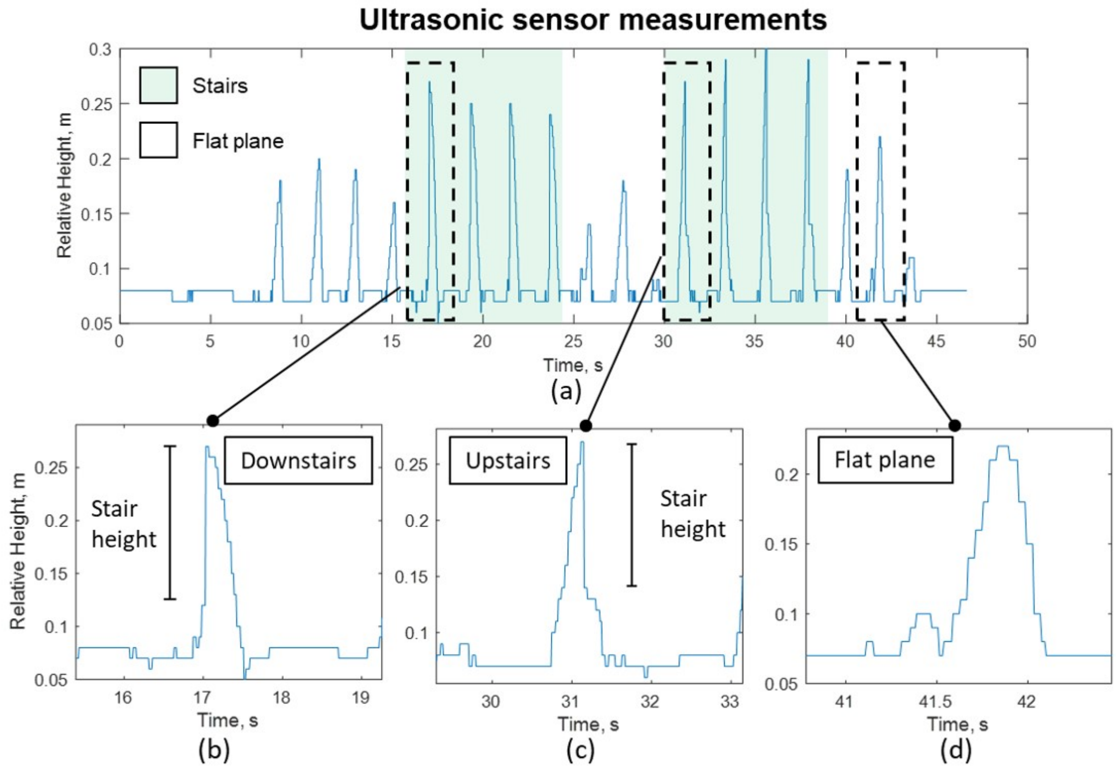

Fig. 2. (a) The ultrasonic measurements collected by a shoe-mounted downward-facing ultrasonic sensor SRF08 during the experiment of walking indoor on flat surfaces, upstairs, and downstairs. The height of each stair was assumed to be nominally identical and was around 15 cm. The total elapsed time in this experiment was 46.5 s. In the period of the first 16 s, 24.5 s to 30.5 s, and 38.5 s to the end, we walked on a flat plane. From 16 s to 24.5 s, we went down four stairs. From 30.5 s to 38.5 s, we went up four stairs to the original height level. (b) ultrasonic profile in the case of downstairs. (c) ultrasonic profile in the case of upstairs. (d) ultrasonic profile in the case of flat plane.

discontinuity in ultrasonic measurements can be observed when the sensor is passing through edges of stairs. These phenomena were observed in indoor walking experiments with the Lab-On-Shoe platform [31] integrated with a downward-facing ultrasonic sensor SRF08 and a barometric altimeter MS5803-01BA, shown in Fig. 1. The sampling rates of the ultrasonic sensor and the barometer were set to 25 Hz and 5 Hz, respectively.

Since distance measurements of the ultrasonic sensor are discretized, two consecutive distinct measurements always have a discontinuity. In the case of walking at a speed of 40 steps per minute on a flat plane, the maximum discontinuity, α, can be approximated as follows:

$$\alpha = \frac{\max(Foot\ relative\ elevation\ )}{F_s \times \frac{T_{swing\ phase}}{2}},$$

where F_s is the ultrasonic sampling rate and $T_{swing\ phase}$ is the swing phase duration. Then, we use the maximum discontinuity α as a threshold to determine smoothness of the measurements. If two consecutive measurements have a difference smaller than the threshold α, then the measurements during this period are considered to be smooth, and vice versa. In this paper, the threshold α is set to 6 cm. Fig. 2(a) presents an example of the ultrasonic measurements collected during an experiment of walking indoor at a speed of 40 steps per minute on flat surfaces, upstairs, and downstairs. In Fig. 2(a), we can see multiple humps in the ultrasonic measurements. Each hump corresponded to the swing phase in a gait cycle. In Fig. 2(b), the first half of the hump had a discontinuity when going downstairs. In Fig. 2(c), when going upstairs, a discontinuity appeared on the second half of the hump. The ultrasonic measurements in the case of walking on flat surfaces, shown in Fig. 2(d), were smooth because there were not any two consecutive measurements that had a difference larger than α.

A. Kalman Filter for Ultrasonic Altimeter

We use a standard Kalman Filter to realize the estimation of the vertical position of the shoe and the floor. The Kalman filter has the following states:

$$\bar{x}_k = [h_k, V_k, L_k]^{\mathrm{T}},$$

where h_k, V_k, and L_k are the shoe height, the shoe vertical velocity, and the floor height in the navigation frame at time k, respectively. In the propagation step of the Kalman Filter, we have the relation $h_{k+1} = h_k + V_k dt$, where dt is the sampling rate of the ultrasonic sensor. Furthermore, we assumed that floor does not move and the shoe velocity in the vertical direction does not change in the propagation step. The propagation matrices F and Q of the Kalman Filter are formulated as follows:

$$F = \begin{bmatrix} 1 & dt & 0 \\ 0 & 1 & 0 \\ 0 & 0 & 1 \end{bmatrix}, Q = \begin{bmatrix} n_{h_k} & 0 & 0 \\ 0 & n_{V_k} & 0 \\ 0 & 0 & n_{L_k} \end{bmatrix},$$

where n_{h_k}, n_{V_k}, and n_{L_k} are the noise corresponding to shoe height, shoe vertical velocity, and floor elevation, modeled as zero-mean Gaussians with respective variances $\sigma^2_{h_k}$, $\sigma^2_{V_k}$, and $\sigma^2_{L_k}$.

In the update step of the Kalman Filter, the ultrasonic sensor provides three types of data: 1) relative distance between the shoe and the floor $d_{k,SONAR}$, which are the raw readouts from the sensor, 2) vertical velocity of the shoe $V_{k,SONAR}$, obtained by subtracting two consecutive ultrasonic measurements, and 3) floor elevation in navigation frame $L_{k,SONAR}$. The ultrasonic measurement of the floor elevation is achieved by observation that a discontinuity Δh is displayed in ultrasonic measurements when the sensor is passing through edges of stairs. The value of the discontinuity Δh, as the ultrasonic sensor scans through edges of stairs, is considered to be the change of floor elevation when both the pitch angle and the vertical velocity of the shoe are very close to zero. A consequence of this configuration is that the value of the floor elevation measurement is equal to the current floor height when no discontinuity is observed, which is the case for flat surfaces. The measurement vector z_k and update matrices H and R of the Kalman filter are formulated as follows:

$$z_k = \begin{bmatrix} V_{k,SONAR} \\ L_{k,SONAR} \\ d_{k,SONAR} \end{bmatrix} = \begin{bmatrix} \frac{(d_{k,SONAR} - d_{k-1,SONAR})}{dt} \\ L_{k-1,SONAR} - \Delta h \\ d_{k,SONAR} \end{bmatrix} = \begin{bmatrix} V_k + n_{V_{k,SONAR}} \\ L_k + n_{L_{k,SONAR}} \\ h_k - L_k + n_{d_{k,SONAR}} \end{bmatrix},$$

$$H = \begin{bmatrix} 0 & 1 & 0 \\ 0 & 0 & 1 \\ 1 & 0 & -1 \end{bmatrix}, R = \begin{bmatrix} n_{V_{k,SONAR}} & 0 & 0 \\ 0 & n_{L_{k,SONAR}} & 0 \\ 0 & 0 & n_{d_{k,SONAR}} \end{bmatrix},$$

where $n_{d_{k,SONAR}}$, $n_{V_{k,SONAR}}$, and $n_{L_{k,SONAR}}$ are the noises corresponding to ultrasonic measurements of shoe relative height, shoe vertical velocity, and floor elevation, modeled as zero-mean Gaussian with respective variances $\sigma^2_{h_{k,SONAR}}$, $\sigma^2_{V_{k,SONAR}}$, and $\sigma^2_{L_{k,SONAR}}$.

B. Performance Evaluation

In this section, we present an example of measurements of an ultrasonic altimeter. We tested the ultrasonic altimeter with the indoor walking experiment discussed in Fig. 2. The initial height was assumed to be 17 m above the sea level. The noise characteristics, determined according to the nominal specification described in the datasheet of the ultrasonic sensor SRF08, were summarized in Table 1. In this experiment, the threshold α for determining the smoothness of the ultrasonic measurements was set to 6 cm. Fig. 3(a) shows the estimated heights of the shoe and the floor, represented by a red curve and a blue curve, respectively. The black curve in Fig. 3(a) illustrates the vertical positions estimated by the standalone ZUPT-aided INS based on IMU measurements collected in the same experiment. Details of the implementation of the standalone ZUPT-aided INS can be found in [6]. In this experiment, the accumulated error along the vertical direction of the standalone ZUPT-aided INS was 14 cm, while the error of the ultrasonic

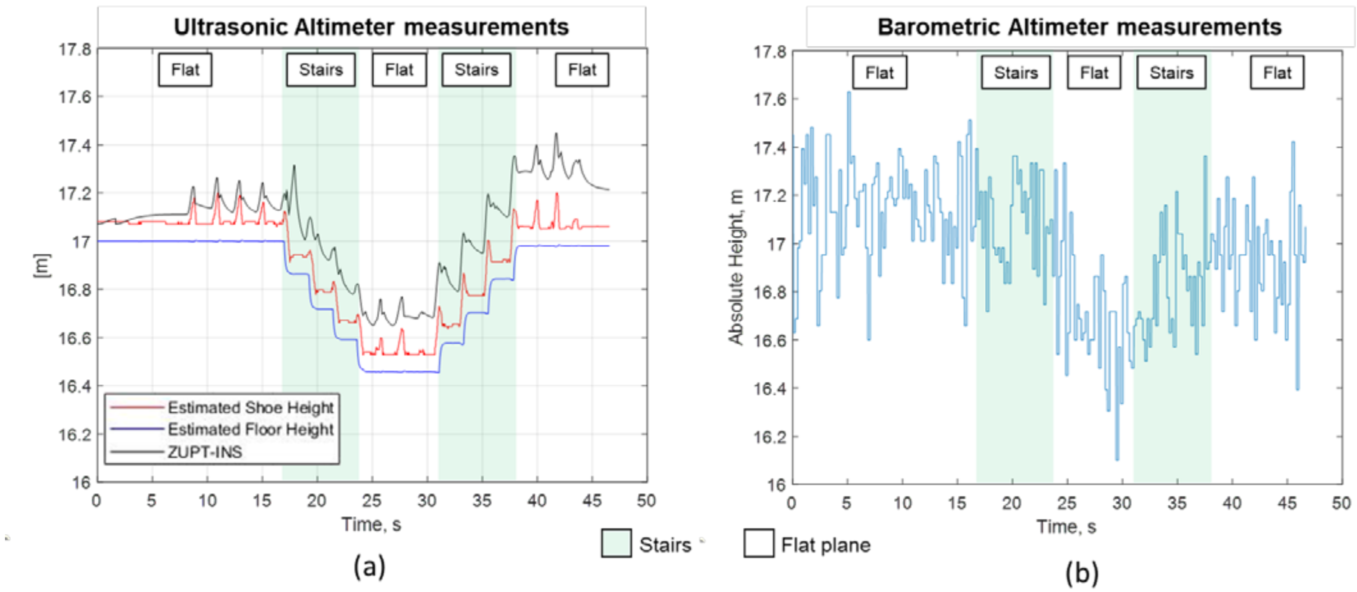

Fig. 3. (a) Shoe height and floor height estimated by the proposed method, and shoe height determined by ZUPT-augmented INS. (b) Barometer readouts collected during the indoor walking experiment.

altimeter decreased to 1 cm. The remaining error sources of the ultrasonic altimeter could be due to 1) limited to resolution of the ultrasonic sensor, and 2) non-zero pitch angle of the shoe when discontinuities were observed, resulting in a shorter estimated floor level change because the sound waves might hit walls of the stairs, instead of ground. Filtering of these multi-path events would require an additional signal processing element.

Noise	n_{h_k}	n_{V_k}	n_{L_k}	$n_{V_{k,SONAR}}$	$n_{L_{k,SONAR}}$	$n_{d_{k,SONAR}}$
Variances	0.01	0.01	0.1	0.01	0.05	1

Table 1. Noise Characteristics of the Kalman Filter for the Ultrasonic Altimeter.

Fig. 3(b) shows the readouts of the barometer MS5803-01BA collected in the same experiments discussed in Fig. 3(a). Two observations can be made as we compare Fig. 3(a) and (b). First, the measurements of ultrasonic altimeter demonstrated a higher resolution than the barometer, which has the lowest resolution among Commercial-Off-The-Shelf sensors. Second, the ultrasonic altimeter captured subtle foot motions, which were not observed in the barometric measurements. The subtle foot motion could benefit the overall navigation results of a pedestrian INS.

III. HYBRID ULTRASONIC/BAROMETRIC ALTIMETER

The hybrid altimeter presented in this section uses both measurements from the ultrasonic altimeter and the barometer. The main reason why the ultrasonic altimeter is not sufficient in its characteristics to replace barometers is that it does not account for other possible terrains that appear in indoor environments, such as ramp or elevator. It fails to operate under such conditions because, in the Kalman Filter for the ultrasonic altimeter discussed in Section IIA, the floor height state is updated only when a discontinuity (or a stair) is detected. When the ultrasonic altimeter operates under a ramp or inside an elevator, the estimated floor elevation will remain the same, which leads to incorrect estimation of the shoe height.

The hybrid altimeter aims to include the ultrasonic altimeter's advantages of stability and high resolution, while also leveraging barometer's capability of operation in the cases of ramp and elevator. Thus, the hybrid altimeter is designed to adaptively select the weight to put on the two types of altimeters based on the terrain under operation and to fuse the two measurements. The adaptive property is achieved with a Multi-Model Kalman Filter, and the detection of different indoor terrains is realized with a foot-mounted IMU. Fig. 4(a) presents the framework for the hybrid altimeter. In the case of flat surfaces or stairs, the measurements from the ultrasonic altimeter receive more weights in the fusion process. When operating inside an elevator or on a ramp, the hybrid altimeter increases the weights of the barometer.

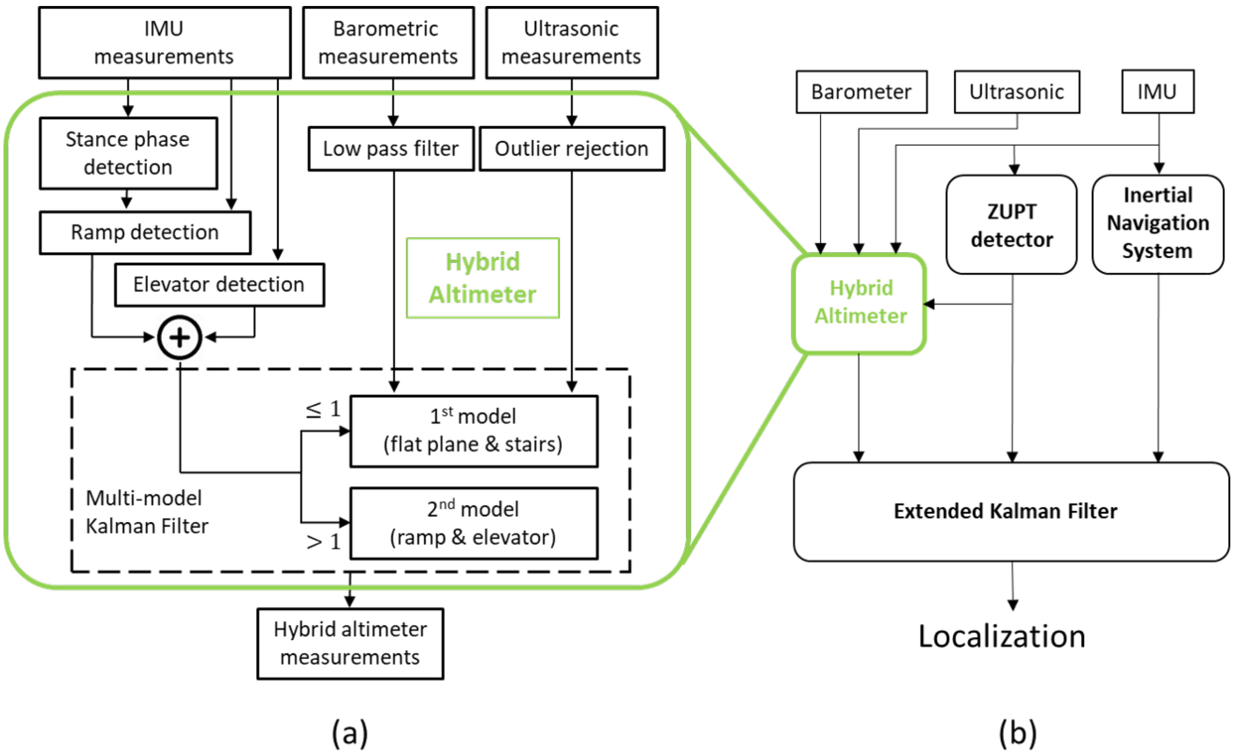

Fig. 4. (a) The framework for the hybrid ultrasonic/barometric altimeter. (b) ZUPT-aided INS augmented by the hybrid altimeter.

Next, we will discuss the principles of the elevator detection and the ramp detection. We will also explain the configuration of the Multi-Model Kalman Filter in detail.

A. Ramp Detection

The detection of ramps in the hybrid altimeter framework is designed to be accomplished by a foot-mounted IMU. An example of using a foot-mounted IMU to detect indoor ramps was introduced in [32]. The detection principle used in this paper is that during the stance phase in a gait cycle, when the motion experienced by an IMU is minimal, the pitch angle of the IMU in the case of ramps is different from the case of flat planes. For example, if the pitch angle of a foot-mounted IMU is zero when the shoe contacts a flat plane, we can determine that the contacting ground is a ramp when the pitch angle of the IMU is not zero. To account for swing phases, we made an assumption that if the foot in the current stance phase rests on an incline, then the foot was traveling over the incline during the entire period of the previous swing phase.

The pitch angle θ of the foot at time k can be directly calculated by accelerometers measurements y_k^a when the foot motion is minimum and can be expressed as follows:

$$\theta(y_k^a) = atan2\left(\frac{y_k^{a,x}}{\sqrt{\left(y_k^{a,y}\right)^2 + \left(y_k^{a,z}\right)^2}}\right),$$

where $y_k^a = \left[y_k^{a,x\mathrm{T}},\ y_k^{a,y\mathrm{T}},\ y_k^{a,z\mathrm{T}}\right]^\mathrm{T}$ and $y_k^{a,x}, y_k^{a,y}$, and $y_k^{a,z}$ are the readouts of the accelerometers along the x, y, and z axis at time k, respectively.

The status of the foot can be determined by a stance phase detector. In this paper, we use the Stance Hypothesis Optimal

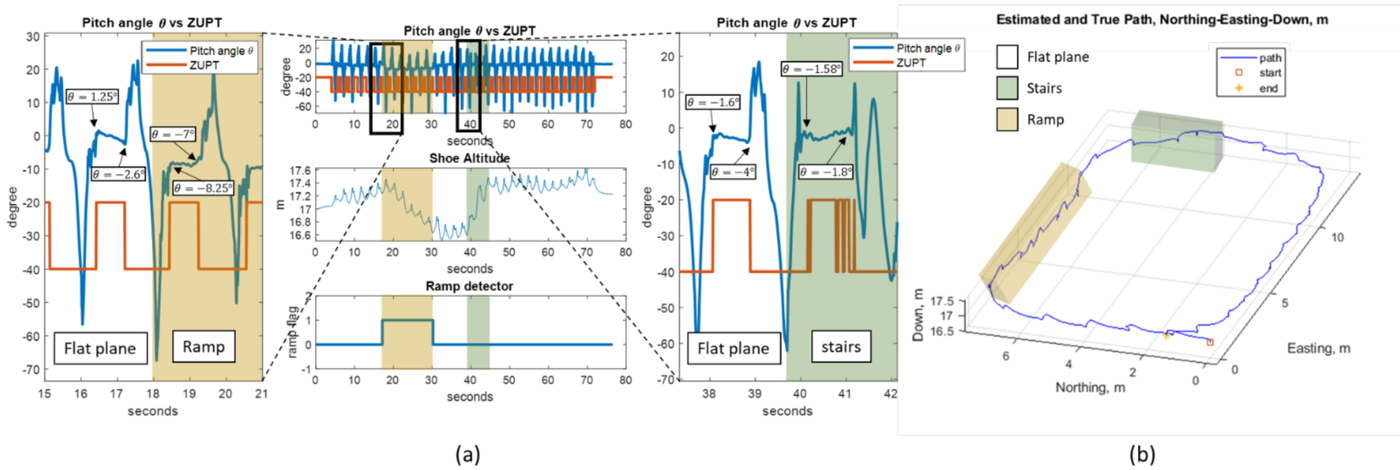

Fig. 5. (a) The pitch angle measurements estimated by accelerometers, the stance phase status, the detected ramp flags, and the reference shoe height estimated by ZUPT-aided INS in the experiment for ramp detection. (b) The reference trajectory, obtained by the ZUPT-aided INS, of the experiment for ramp detection.

dEtection (SHOE) detector [33], which determines a stance phase if

$$T(z_n) = \frac{1}{N}\sum_{k\in\Omega_n}\left(\frac{1}{\sigma_a^2}\left|y_k^a - g\frac{\bar{y}_k^a}{|\bar{y}_k^a|}\right|^2 + \frac{1}{\sigma_\omega^2}|y_k^\omega|^2\right) < \gamma,$$

where $\Omega_n = \{l \in \mathbb{N}, \mathrm{n} \le \mathrm{l} \le \mathrm{N}-1\}$ is a collection of the IMU measurement indexes at time n with a window of length N, $z_n = \left\{\left[y_k^{a\,\mathrm{T}}, y_k^{\omega\,\mathrm{T}}\right]^{\mathrm{T}}\right\}_{k=n}^{k=N-1}$ is a sequence of the IMU measurements in the window, y_k^ω are the gyroscope measurements at k, σ_a^2 is the noise variance of the accelerometer, σ_ω^2 is the noise variance of the gyroscope, and γ are user-defined thresholds.

Combining the pitch angle calculated from IMU measurements and stance phase detection, the ramp detector T_{ramp} can be formulated as follows:

Ramp detection
$l =$ The last stance phase
if $T(z_n) < \gamma$ **then**
if $|\theta(y_n^a) - \theta_0| < \epsilon$ **then**
$T_{ramp}(z_n) = 1$
if $T_{ramp}(z_l) == 1$ **then**
$k = l + 1$
while $k \le n$ **do**
$T_{ramp}(z_k) = 1$
$k = k + 1$
end while
end if
else
$T_{ramp}(z_n) = 0$
end if
else
$T_{ramp}(z_n) = 0$
end if
$n = n + 1$

where θ_0 is the pitch angle obtained at the beginning of the experiment when the foot was the on the ground. The parameter ϵ is a threshold used here to improve the robustness of the detector since the estimated pitch angle in practice is rarely exactly equal to zero. $T_{ramp}(z_k) = 1$ indicates that a ramp is detected at time k.

To test the performance of the developed ramp detector, we conducted a close-loop experiment with trajectory that included flat surfaces, stairs, and a ramp. Fig. 5(b) shows the reference trajectory obtained from the standalone ZUPT-aided INS. In the experiment, the agent first walked towards the North for 7 meters on a flat surface in 16 seconds, turned 90° to the East and walked

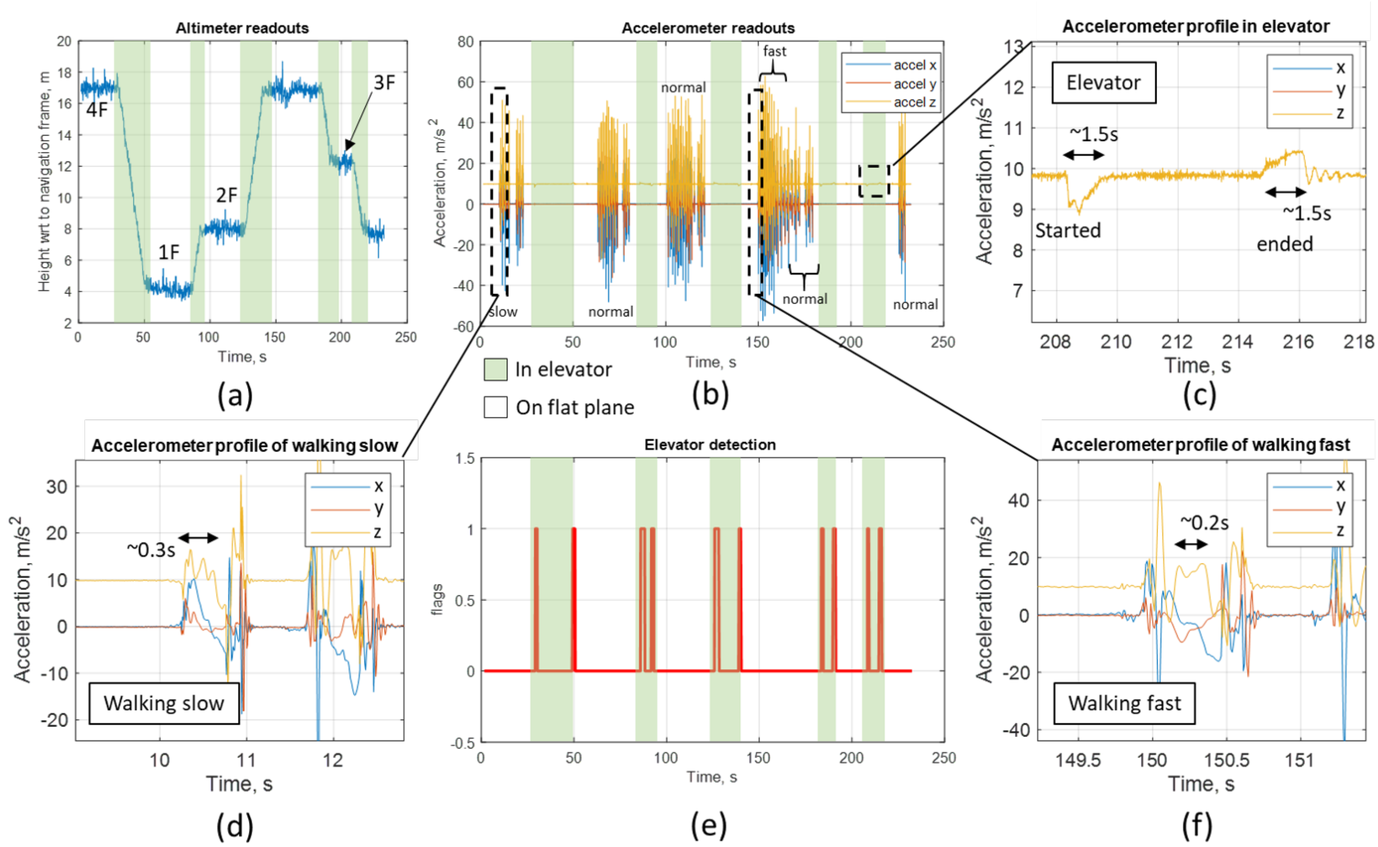

Fig. 6. (a) The reference vertical trajectory, estimated by the barometer, of the experiment for elevator detection. (b) The accelerometer measurements collected during the experiment. (c) Acceleration profiles of the start and the end of the elevator motion. (d) Acceleration profiles of walking slowly. (e) The elevator detection results of the experiment. (d) Acceleration profiles of walking fast.

for 13 meters in 12 seconds on a ramp, turned 90° to the South and walked upstairs for three steps in 5 seconds, proceeded with walking on a flat surface for 6 meters in 10 seconds, turned 90° to the West and walked back to the starting point on a flat surface.

Fig. 5(a) shows the pitch angle measurements, the stance phase status, the detected ramp flags, and the reference shoe height estimated by ZUPT-aided INS. The left-hand side of Fig. 5(a) presents a zoomed-in view that includes two gait cycles in the experiments. The gait during $16s$ to $18\ s$ was on a flat surface, and the one during $18\ s$ to $21.2\ s$ was on a ramp. A clear difference between the pitch angles during the two stance phases can be observed. The pitch angles in the case of a flat plane ranged from $-2.6°$ to $1.25°$, while in the case of ramp, the range was from $-7°$ to $-8.25°$. The right-hand side of Fig. 5(a) presents another zoomed-in view that includes two other gait cycles in the experiments. The gait during $38\ s$ to $39.5\ s$ was on a flat surface, and the one during $39.5\ s$ to $41\ s$ was on a stair. The detected pitch angles when foot rested on the flat plane and the stair had similar values, both had the range between $-4°$ to $-1.6°$. The discussed ramp detector with a $\epsilon = 4°$ achieved a 100 % accuracy rate and no false alarm in this experiment.

B. Elevator Detection

Elevator detection can be achieved with the z-axis accelerometer of a foot-mounted IMU. An example of elevator detection using the z-axis accelerometer was presented in [34]. The detection concept is that when a person with a foot-mounted IMU is standing inside a moving elevator the direction of the force experienced by the IMU within a period of time is consistent, while in the same length of time, the direction of the force generated by foot dynamics is inconsistent. Fig. 6(c), (d), and (f) illustrate examples of vertical accelerations measured by the Lab-On-Shoe platform in the cases of walking slowly, walking fast, and standing inside a moving elevator. In Fig. 6(d) and (f), we can see that the period of time when the IMU is experiencing the same direction of acceleration was $0.3s$ in the case of walking slowly and $0.2s$ in the case of walking fast. In Fig. 6(c), the period of time that the IMU experienced acceleration from the same direction was $1.5s$. Thus, the elevator detection can be achieved by observing a window with length N of the z-axis accelerometer measurements. If all the measurements within the window are consistently larger or consistently smaller than the gravity, then the motion is generated by the elevator instead of the foot. The detection mechanism can be described as follows:

Elevator detection	
1	**if** $y_k^{a,z} < g \ \forall k \in \Omega_n$ **or** $y_k^{a,z} > g \ \forall k \in \Omega_n$ **then**
2	$\quad T_{elevator}(z_n) = 1$
3	**else**
4	$\quad T_{elevator}(z_n) = 0$
5	**end if**

where $\Omega_n = \{l \in \mathbb{N}, \mathrm{n} \leq \mathrm{l} \leq \mathrm{N} - 1\}$ is a collection of the IMU measurement indexes at time n with a window of length N, $z_n = \left\{\left[y_k^{a\mathrm{T}}, y_k^{\omega\mathrm{T}}\right]^{\mathrm{T}}\right\}_{k=n}^{k=N-1}$ is a sequence of the IMU measurements in the window, and $y_k^{a,z}$ is the z-axis accelerometer measurement at time k.

To test the performance of the elevator detector, we conducted an indoor experiment, including walking and standing in a moving elevator. In the experiment, the subject started from the fourth floor of a four-story building and walked into the elevator. During $17s$ to $51s$, $86s$ to $92s$, $126s$ to $140s$, $185s$ to $191s$, and $208s$ to $218s$, the subject was standing inside the moving elevator. The periods between $51s$ and $86s$, $92s$ and $126s$, $140s$ and $185s$, the subject moved out of the elevator, walked around on a flat surface, and went back into the elevator. During $191s$ and $208s$, the subject stood inside of the still elevator. The total time duration of the experiment was $232s$. The vertical trajectory of the subject was illustrated by a barometer, shown in Fig. 6(a). Fig. 6(b) demonstrates the accelerometer measurements collected during the experiment and Fig. 6(e) presents the detection results. In this experiment, we set the window of length to be $1s$. The detection of elevator motion achieved 100% detection rate with no false alarm.

C. Multi-Model Kalman Filter for the Hybrid Altimeter

The hybrid altimeter uses both ultrasonic and barometric altimeters. Since barometric measurements have a bias that comes from ambient weather changes, the bias also needs to be estimated. We augment the Kalman Filter state discussed in Section IIA with a bias state b_k for the barometer. The augmented Kalman Filter states are formulated as follows:

$$\bar{x}_k = [h_k, V_k, L_k, b_k]^{\mathrm{T}},$$

In the propagation step of the Multi-Model Kalman Filter, we assumed that the bias state b_k, whose noise n_{b_k} is modeled as a Gaussian distribution, maintains the same expected value. The dynamics of the other states is inherited from the Kalman Filter for the ultrasonic altimeter. Thus, we can express the propagation matrices F and Q of the Kalman Filter as follows:

$$F = \begin{bmatrix} 1 & dt & 0 & 0 \\ 0 & 1 & 0 & 0 \\ 0 & 0 & 1 & 0 \\ 0 & 0 & 0 & 1 \end{bmatrix}, Q = \begin{bmatrix} n_{h_k} & 0 & 0 & 0 \\ 0 & n_{V_k} & 0 & 0 \\ 0 & 0 & n_{L_k} & 0 \\ 0 & 0 & 0 & n_{b_k} \end{bmatrix}.$$

The barometer readout $h_{k,baro}$ is considered as the summation of true heights h_k, current sensor bias b_k, and a Gaussian noise $n_{h_{k,baro}}$ with variance $\sigma_{h_{k,baro}}^2$, which can be expressed as:

$$h_{k,baro} = h_k + b_k + n_{h_{k,baro}}.$$

In the update step of the Multi-Model Kalman Filter for the proposed hybrid altimeter, we augmented the measurement vector z_k of the Kalman Filter for the ultrasonic altimeter with the height measurement $h_{k,baro}$ from the barometer. The measurement vector z_k of the Multi-model Kalman Filter is expressed as:

$$z_k = \begin{bmatrix} h_{k,baro} \\ V_{k,SONAR} \\ L_{k,SONAR} \\ d_{k,SONAR} \end{bmatrix},$$

and the corresponding measurement matrices H and R are formulated as follows:

$$H = \begin{bmatrix} 1 & 0 & 0 & 1 \\ 0 & 0 & 1 & 0 \\ 0 & 0 & 0 & 1 \\ 0 & 1 & 0 & -1 \end{bmatrix}, R = \begin{bmatrix} n_{h_{k,baro}} & 0 & 0 & 0 \\ 0 & n_{V_{k,SONAR}} & 0 & 0 \\ 0 & 0 & n_{L_{k,SONAR}} & 0 \\ 0 & 0 & 0 & n_{d_{k,SONAR}} \end{bmatrix},$$

The Multi-Model Kalman Filter has two models. The two models differ in the noise characteristics of the states h_k, V_k, L_k, and b_k and the measurements $V_{k,SONAR}$ and $L_{k,SONAR}$. In the first model, where the altimeter is assumed to operate over flat surfaces and ramps, the noise variance configuration, except for the states b_k, is the same as in the case of the ultrasonic altimeter. As for the state b_k, since it is equivalent to $h_{k,baro} - h_k$ and the state h_k in the first model is mainly affected by the ultrasonic altimeter, the noise variance is set to a value comparable to the maximum distance measured by the ultrasonic sensor. In the second model, which is the case of elevators and ramps, the noise characteristics of the states h_k, V_k, and L_k and the measurements $V_{k,SONAR}$ and $L_{k,SONAR}$ are increased because under these terrains, the ultrasonic altimeter does not provide reliable measurements. The noise variance of the state b_k, on the other hand, is set to a value that was experimentally determined. This value is usually much lower than the value in the first model. Table 2 summarizes the values used in this paper for the noise characteristics of the Multi-Model Kalman Filter.

Noise	n_{h_k}		n_{V_k}		n_{L_k}		$n_{V_{k,SONAR}}$		$n_{L_{k,SONAR}}$		$n_{d_{k,SONAR}}$		n_{b_k}		$n_{h_{k,baro}}$	
Model	1st	2nd	1st	2nd	1st	2nd	1st	2nd	1st	2nd	1st	2nd	1st	2nd	1st	2nd
Variances	0.01	100	0.01	10	0.1	1	0.01	10	0.05	10	1	1	1	0.01	1	1

Table 2. Noise Characteristics of the Multi-Model Kalman Filter for the Hybrid Altimeter

The framework presented in Fig. 4(a) also includes a low-pass filter for barometer measurements and an outlier rejector module for ultrasonic measurements. The low-pass filter is included because raw measurements of the barometer contain high-frequency thermal and electronic noises. The outlier rejector module is designed to improve the false alarm rate for the stair detection. Machine learning techniques have the potential to classify different gait motion phases based on the ultrasonic altimeter readouts and can be expected to improve the stair detection further.

IV. EXPERIMENTAL VERIFICATION OF THE HYBRID ALTIMETER

To validate the proposed hybrid altimeter, we conducted three series of experiments using the Lab-On-Shoe platform, shown in Fig. 1. In every experiment, the sampling rates of the IMU, barometer, and the downward-facing ultrasonic sensor were set to $120Hz, 5Hz,$ and $25Hz$, respectively. The first series of experiments illustrated that the hybrid altimeter is more robust to temperature and air pressure variations than a conventional barometer. In the second series of experiments of walking on a flat plane, we demonstrated that when estimating a vertical displacement, the accuracy of the ZUPT-based INS aided by a hybrid altimeter outperformed both ZUPT-aided INS cases, standalone and barometer-aided. The third series of experiments investigated the performance of the ZUPT-based INS aided by the hybrid altimeter when walking on different terrains, such as flat surfaces, stairs, ramps, and elevators.

A. Experiments when barometer is subject to temperature and air pressure changes

To investigate robustness of the hybrid altimeter measurements when the barometer is subjected to variations due weather changes, we conducted an experiment simulating an environment where surrounding temperature and air pressure are unstable. The nominal trajectory of the experiment is shown in Fig. 7(a), which was obtained by a standalone ZUPT-aided INS. A subject started the navigation from a reference position in the hallway and the trajectory was recorded by the Lab-On-Shoe platform. The subject started to walk $10\ m$ towards the South. At the 60 s mark, the subject stopped and during this time a fire was simulated by heating up the

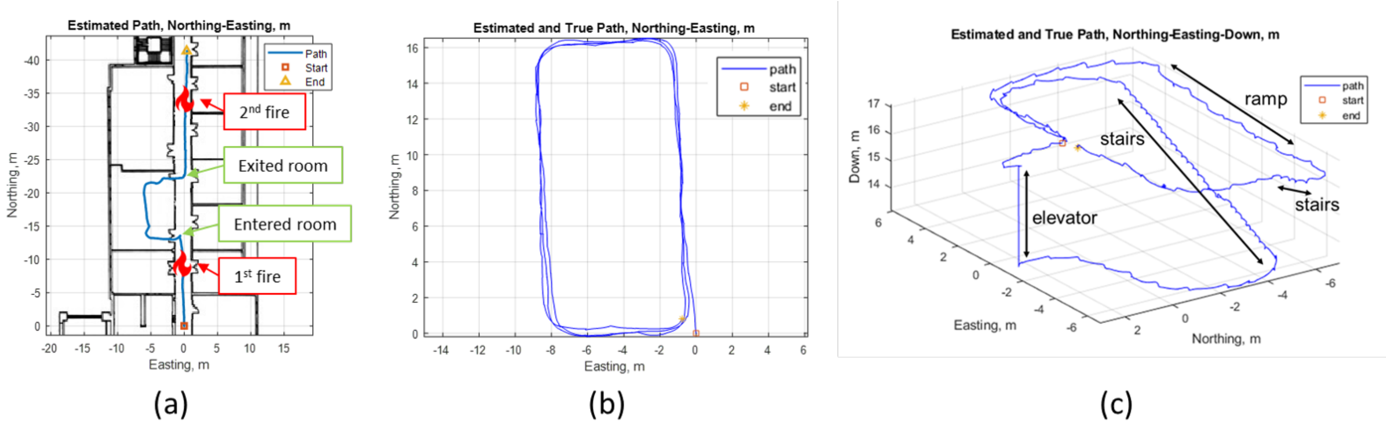

Fig. 7. (a) Reference trajectory for the experiments when barometer is subject to temperature and air pressure changes. (b) Reference trajectory for the indoor experiment walking on a flat plane. (c) Reference trajectory for the indoor experiment walking on different terrains.

barometer for $0.1\ s$ with a commercial lighter. The subject continued the navigation and entered a room at $78\ s$, walked for $8\ m$, and left the room at $100\ s$. Then, the subject walked for another $10\ m$ towards the South and stopped at $120\ s$. At $140\ s$, another heat source lasting $0.1\ s$ was triggered next to the barometer. The subject moved toward the South for another $7\ m$ to reach the destination. The time duration of this experiment was $180\ s$, and the nominal heights of the starting point and the ending point were the same. In the experiment, the subject walked at a speed of approximately 40 steps per minute. Next we analyze the results.

Fig. 8(a) shows the shoe height estimated by the barometer and Fig. 8(b) demonstrates the shoe height and the floor height estimated by the hybrid altimeter. In Fig. 8(a), we illustrate that the first fire and the second fire caused vertical errors of $20\ m$ and $13\ m$ for the barometer, respectively. Fig. 8(c) is a zoomed-in view of the sensor measurements during $70\ s$ and $110\ s$, showing that the transitions between the hallway to the room led to the vertical errors of $1\ m$ and $1.2\ m$, as judged from measurement of the barometer. In Fig. 8(b), we demonstrated that the two events of fire and the transitions between different rooms had a minimal effect on the hybrid altimeter measurements. Fig. 8(b) depicts that the hybrid altimeter can capture subtle foot motions while the barometer is incapable of capturing the motions due to insufficient resolution.

This experiment investigated the effect of air pressure and temperature changes on readings of the barometers. The operational principle of the ultrasonic sensor involves transmission of the sound wave in air, which is affected by the changes in ambient air pressure and temperature. This effect was not accounted in these experiments.

B. Experiments of walking on flat planes

To derive the performance of the hybrid altimeter, when used to assist the ZUPT-aided INS, we first performed experiments of walking indoor at a speed of approximately 40 steps per minute in a square shape pattern for three full circles. We repeated the same experiment 10 times. In the experiment, the starting position and the ending position were the same. The total trajectory length was $150\ m$, and the navigation time was $232\ s$. The experiment was conducted on the same floor, so there was no floor height changes during the entire experiment. We assumed that the initial height was $17m$ above the sea level. Fig. 7(b) shows a nominal horizontal trajectory obtained by the ZUPT-aided INS. Since the altimeter measurements do not have significant impacts on the displacement errors along the horizontal directions, we only focused on errors along the vertical direction. We used the ZUPT-aided INS augmented by an altimeter for localization, as described in [18]. Note, that the altimeter used in [18] was a barometer but the same analytical framework can be applied when the barometer is replaced by the proposed hybrid altimeter. Fig. 4(b) illustrates the configuration of the ZUPT-aided INS augmented by the hybrid altimeter.

Fig. 9(a) shows the estimated height measurements from 1) standalone ZUPT-based INS, 2) ZUPT-based INS aided by the barometer, and 3) ZUPT-based INS aided by the hybrid altimeter. Fig. 9(b) shows the final vertical displacements of the 10 sets of experiments estimated by the three different navigation solutions. The red horizontal line in Fig. 9(b) indicates the true height. We calculated the Root Mean Square Error (RMSE) based on the 10 sets of the experiment, summarized in Table 3, and found that the RMSEs of the standalone ZUPT-based INS, the ZUPT-based INS aided by the barometer, and the ZUPT-based INS aided by the hybrid altimeter

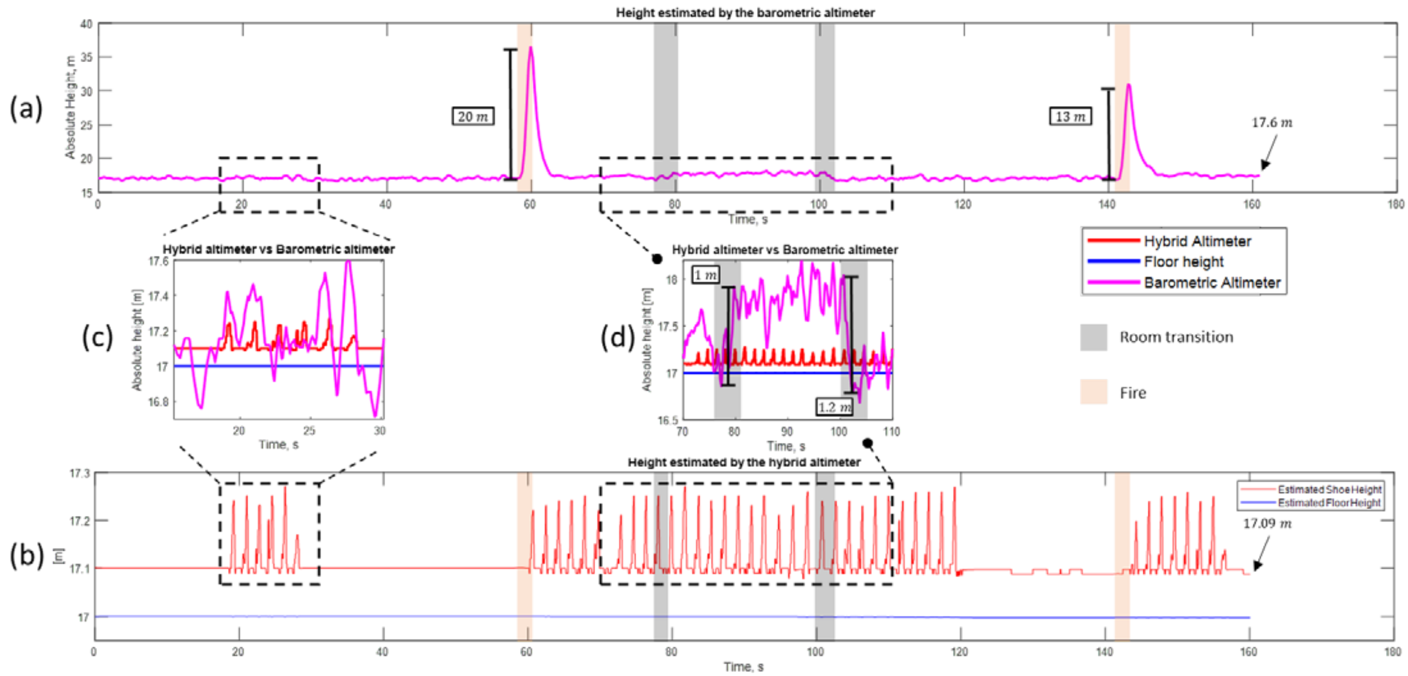

Fig. 8. (a) The height, measured by the barometer, of the experiment discussed in Section IVA. (b) The height measured by the hybrid altimeter of the experiment. (c) Comparison of the two altimeters in walking in an environment with stable air pressure and temperature. The hybrid altimeter could capture the subtle foot motion while the barometer failed to do so. (d) Comparison of the two altimeters in the case of air pressure changed due to the room transition. The height measured by the barometer was affected by the transition while the measurement of the hybrid altimeter maintained stable.

were $0.27\ m$, $0.453\ m$, and $0.01\ m$, respectively. In this series of experiments, the ZUPT-based INS aided by the hybrid altimeter reduced the error by 96%, as compared to the standalone ZUPT-based INS, and by 97%, as compare to the ZUPT-based INS aided by the barometer.

INS aiding methods	**ZUPT**	**ZUPT + Barometer**	**ZUPT + Hybrid altimeter**
RMSE [m]	0.272	0.453	0.01

Table 3. RMSEs of a standalone ZUPT-based INS, ZUPT-based INS aided by the barometer, and ZUPT-based INS aided by the hybrid altimeter in the experiments of walking on a flat plane.

C. Experiments of walking on different terrains

To demonstrate the hybrid altimeter in a more realistic situations, we conducted a series of experiments with a nominal trajectory that included an elevator, a ramp, flat surfaces, and stairs. The total navigation time in each experiment was $210s$, and the length was $92m$. We repeated 10 sets of the identical experiment. Fig. 7(c) demonstrates a reference trajectory of the experiment obtained by the ZUPT-aided INS augmented by the hybrid altimeter. At the beginning of each experiment, an agent who wore the Lab-On-Shoe platform would start the experiment on the second floor of a building. In the first $33\ s$, the subject moved from the starting point to an elevator. Between $33\ s$ and $41\ s$, the elevator moved down one floor, whose nominal height was measured to be $3.8\ m$. From $41\ s$ to $70\ s$, the subject moved out of the elevator and walked on a flat surface to stairs. Between $70\ s$ to $135\ s$, the subject walked upstairs for 26 stairs. The nominal height of each of the stairs was $15\ cm$. After the first eight stairs, there was a small area of a flat surface, where the subject walked one step during $100\ s$ to $102\ s$ time interval. Between $135\ s$ and $145\ s$, the subject walked on a flat surface to a ramp. From $145\ s$ to $165\ s$, the subject walked down along the ramp. The nominal height difference between the two ends of the ramp was $60\ cm$. From $165\ s$ to $175\ s$, the subject moved on a flat surface to other stairs. From 175 s to $182\ s$, the subject walked upstairs for four stairs. The nominal height of each of the stairs was measured to be $15\ cm$. From $182\ s$ to the end of the experiment, the subject walked back to the starting point on a flat surface. In this series of experiments, the subject walked at a speed of approximately 40 steps per minute. Next, we discuss the results of this experiment.

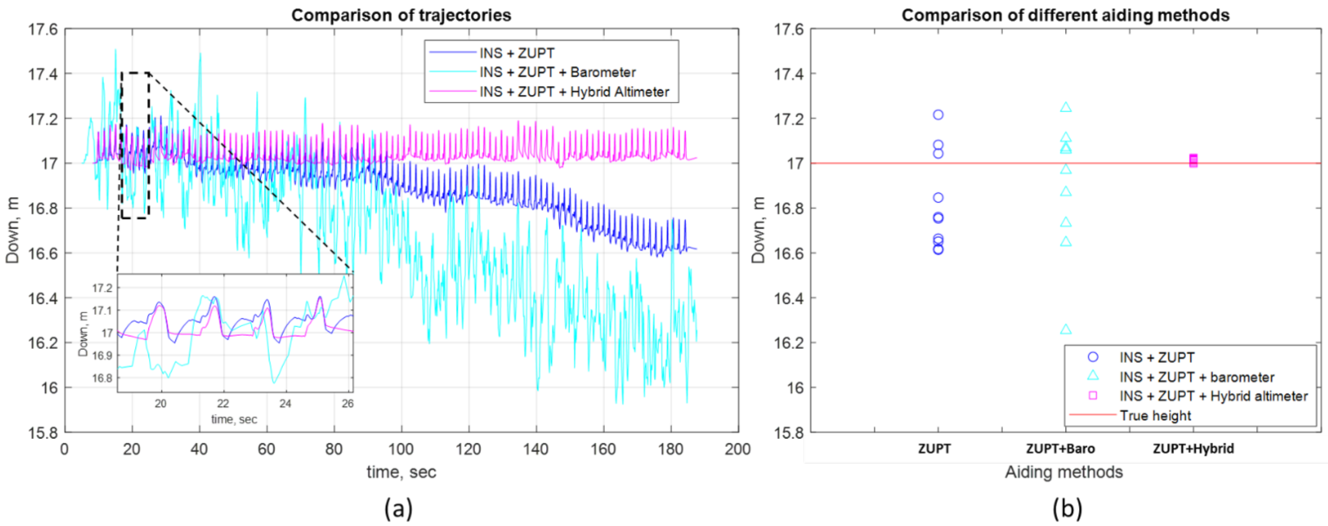

Fig. 9. (a) An example of the height estimated by a standalone ZUPT-based INS, ZUPT-based INS aided by a barometer, and ZUPT-based INS aided by a hybrid altimeter in the experiments presented in Section IVB. (b) Vertical displacement accuracy of all three navigation solutions.

We compared vertical displacements estimated by the ZUPT-augmented INS, the ZUPT-augmented INS aided by the barometer, and the ZUPT-augmented INS aided by the hybrid altimeter. We should point out that because of the stair height estimation error of the ultrasonic altimeter discussed in Section IIB, we applied a constant to compensate stair height estimation. In this series of experiments, we found that the average value of the estimated stair heights was $11.5\ cm$, which was $3.5\ cm$ less than the nominal stair height. Thus, the compensation value was selected to be $3.5\ cm$ in this series of experiments. The results of three navigation solutions are shown in Fig. 10(a), (b), and (c), respectively. The final vertical displacements of the 10 sets of the experiments for the three navigation solutions are shown in Fig. 10(d). The RMSEs of the three methods summarized in Table 4. In Fig. 10(a), we illustrate that standalone ZUPT-augmented INS could not account for the elevator motion, leading to identification of a wrong floor. Although in this series of experiments, the RMSE of the ZUPT-augmented INS aided by the barometer was smaller than when aided by the hybrid altimeter, instability in the estimated height profiles can be observed in the case with the barometer. For example, in Fig. 10(b), during $41s$ and $75s$, the ZUPT-augmented INS aided by the barometer indicated that the subject was under the ground level. The primary error sources of the hybrid altimeter were: 1) barometer bias when operating on a ramp or in an elevator and 2) stair height estimation error from the ultrasonic altimeter. The contributing factors of the stair height estimation error were discussed in Section IIB.

INS aiding methods	ZUPT	ZUPT + Barometer	ZUPT + Hybrid altimeter
RMSE [m]	4.15	0.21	0.36

Table 4. RMSEs of the standalone ZUPT-based INS, ZUPT-based INS aided by the barometer, and ZUPT-based INS aided by the hybrid altimeter in the experiments of walking on different terrains, including flat surfaces, a ramp, stairs, and an elevator.

D. Discussion

In Section IVA, IVB, and IVC, we have demonstrated that the proposed hybrid altimeter can achieve accurate estimation of vertical displacement when operating under different terrains. However, we identified two major challenges when using the proposed hybrid altimeter.

1) Stair height underestimate. In our opinion, the underestimate is mainly contributed from three factors: 1) multi-path effects of ultrasonic sensors, 2) the fact that the vertical velocity of the foot when going above the edges of stairs is not zero, and 3) wide detection cone of the ultrasonic sensor SRF08 resulting in detecting the wall of stairs when scanning through the edge of the stairs. The first factor could possibly be resolved by including an additional signal processing module in the hybrid altimeter framework. To address the second factor, additional velocity detectors are required. The third factor can be potentially eliminated by using a range sensor that has a narrow detection cone, such as LiDAR. The underestimate of stair height also implies that the assumption of the state L_k for floor height and the measurement $L_{k,SONAR}$ being zero-mean Gaussian random variables might be inaccurate.

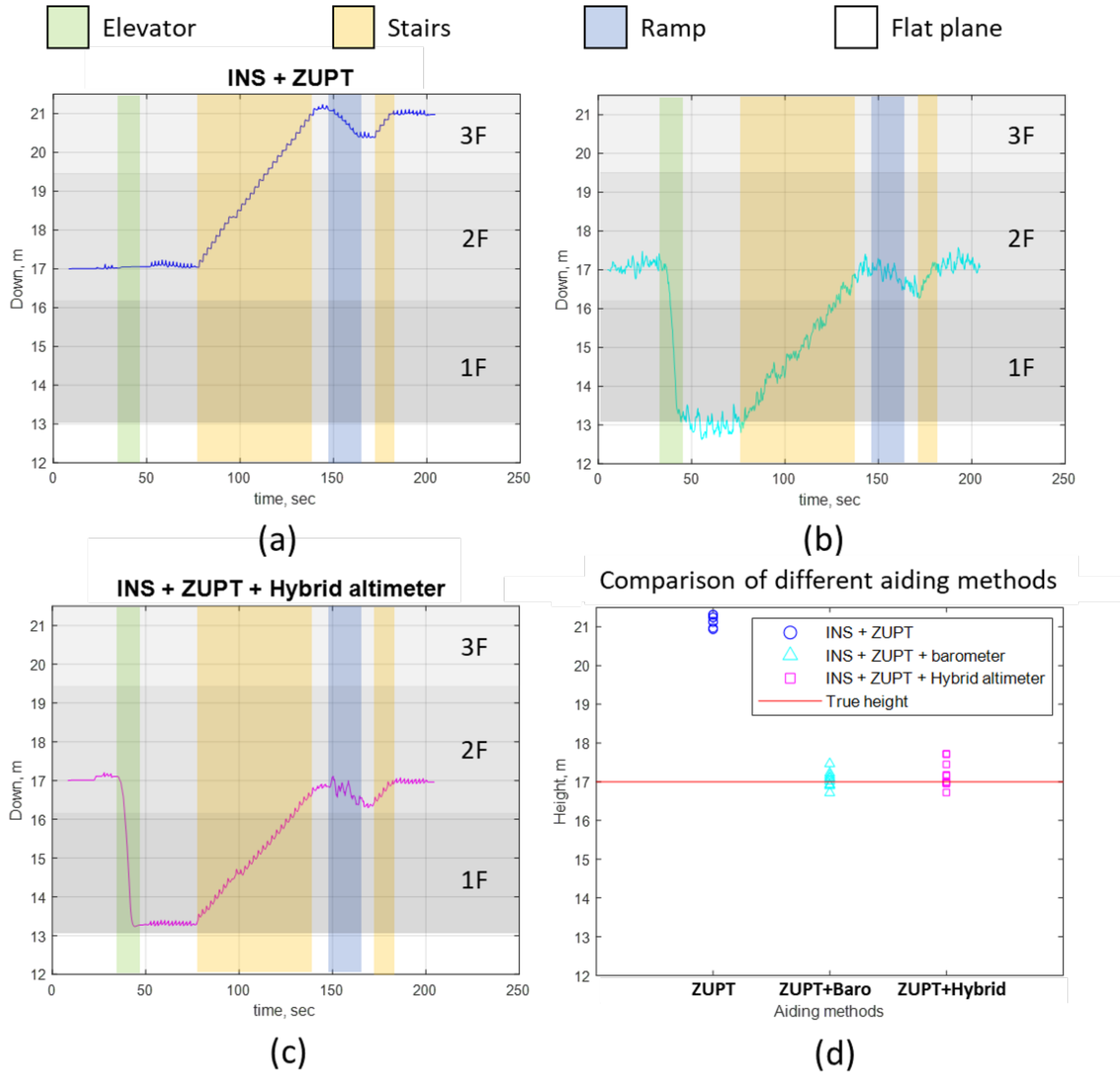

Fig. 10. (a), (b), and (c) examples of the height estimated by standalone ZUPT-based INS, ZUPT-based INS aided by the barometer, and ZUPT-based INS aided by the hybrid altimeter in the experiments presented in Section IVC. (d) The final vertical displacements of the three navigation solutions.

2) False alarms of stairs detection. In the ultrasonic altimeter module, we defined a threshold for determining the smoothness of the ultrasonic measurements, and if the measurement is not smooth, or equivalently has a discontinuity, then a stair is detected. However, due to the low sampling rate of the ultrasonic sensor, in the case of walking fast or running, two consecutive ultrasonic measurements tend to have a difference larger than the smoothness threshold, even when walking on a flat plane. The large difference can result in false alarms of stair detection. This phenomenon could be reduced if an array of sensors with a high sampling rate is used. Another contributing factor to false alarms of stair detection is related to walking patterns. We observed that in some gait patterns, there is a short period during the swing phase that the bottom of the foot is facing the surrounding wall of a building, instead of the ground. This phenomenon would result in two significant discontinuities in the ultrasonic measurement collected during this period. One is a positive discontinuity at the beginning of the period, and the other is a negative one at the end of the period. Our solution to this problem was to use a temporal

threshold to determine a false alarm of the stair detection if the time difference between occurrences of a positive and negative discontinuities is smaller than the temporal threshold.

V. CONCLUSION

In this paper, we proposed a hybrid altimeter that uses a barometer and a downward-facing ultrasonic altimeter for aiding foot-mounted INS. The development of the hybrid altimeter aims to minimize the usage of barometric altimeter in height estimation as measurements of barometers are easily affected by ambient temperature and air pressure changes. We first showed that a shoe-mounted downward-facing ultrasonic sensor alone could be used as an altimeter, in the case of flat surfaces and stairs, by simultaneously estimating shoe height and floor elevation. To account for other common indoor terrains, such as ramps and elevators, we use a Multi-Model Kalman Filter to fuse measurements of the barometer and the ultrasonic altimeter. In the fusion process, the hybrid altimeter adaptively selects weights for the two altimeters based on the terrains under operation. In the cases of flat planes and stairs, the ultrasonic altimeter has high-resolution and stable measurements, thus the noise variances corresponding to the ultrasonic altimeter are set to lower values than the noise variance of the barometer. In the case of ramps and elevators, the barometer measurements are more reliable than the ultrasonic sensor; therefore, the noise variances of the barometer are decreased, and those of the ultrasonic altimeter are increased. Detection of elevators and ramps were shown in this paper to be achieved with a foot-mounted IMU. Three series of experiments were conducted to test the performance of the proposed hybrid altimeter. The first experiment showed that the hybrid altimeter was less sensitive to temperature and air pressure changes in the surrounding environment, as compared to the barometer. The second series of experiments investigated the performance of the hybrid altimeter in the case of walking slowly on a flat plane, and experimental results indicated that the ZUPT-based INS aided by the hybrid altimeter improved the RMSE along the vertical direction by 96%, as compared to a standalone ZUPT-based INS, and by 97%, as compared to the ZUPT-based INS aided by the barometer. In the third series of experiments, we validated the operation of the hybrid altimeter in the cases of common indoor terrains, such as flat surfaces, stairs, ramps, and elevators. The experimental results showed that the RMSE of the ZUPT-based INS aided by the hybrid altimeter outperformed the RMSE of the standalone ZUPT-based INS by 91%. When compared to the RMSE of the ZUPT-based INS aided by the barometer, the RMSE of the ZUPT-based INS aided by the hybrid altimeter was increased by 41% ($0.15\ m$). In our opinion, the primary sources contributing to the vertical error of the ZUPT-based INS aided by the hybrid altimeter are the underestimate of stair height and the false alarm of stair detection of the ultrasonic altimeter.

ACKNOWLEDGMENTS

This work is performed under the following financial assistance award: 70NANB17H192 from US department of Commerce, National Institution of Standards and Technology (NIST).

REFERENCES

[1] Y. Chen, R. Chen, L. Pei, T. Kröger, H. Kuusniemi, J. Liu and W. Chen, "Knowledge-based error detection and correction method of a multi-sensor multi-network positioning platform for pedestrian indoor navigation," in *IEEE/ION Position, Location and Navigation Symposium*, Indian Wells, CA, USA, 2010.

[2] L. Chen, H. Kuusniemi, Y. Chen, L. Pei, T. Kröger and R. Chen, "Motion restricted information filter for indoor bluetooth positioning," *International Journal of Embedded and Real-Time Communication Systems (IJERTCS),* vol. 3, pp. 54-66, 2012.

[3] A. Abdallah, K. Shamaei and Z. Kassas, "Indoor Localization with LTE Carrier Phase Measurements and Synthetic Aperture Antenna Array," in *ION GNSS,* Miami, 2019.

[4] E. Foxlin, "Pedestrian tracking with shoe-mounted inertial sensors," *IEEE Computer graphics and applications,* pp. 38-46, 2005.

[5] Y. Wang, A. Chernyshoff and A. M. Shkel, "Error analysis of ZUPT-aided pedestrian inertial navigation," in *International Conference on Indoor Positioning and Indoor Navigation (IPIN),* Nantes, 2018.

[6] Y. Wang, D. Vatanparvar, A. Chernyshoff and A. M. Shkel, "Analytical Closed-Form Estimation of Position Error on ZUPT-Augmented Pedestrian Inertial Navigation," *IEEE Sensors Letters,* vol. 2, pp. 1-4, 2018.

[7] Y. Wang, S. Askari and A. M. Shkel, "Study on Mounting Position of IMU for Better Accuracy of ZUPT-Aided Pedestrian Inertial Navigation," in *IEEE International Symposium on Inertial Sensors and Systems (INERTIAL),* Naples, 2019.

[8] Y. Wang and A. M. Shkel, "Adaptive threshold for zero-velocity detector in ZUPT-aided pedestrian inertial navigation," *IEEE Sensors Letters,* vol. 3, pp. 1-4, 2019.

[9] Y. Wang, S. Askari, C.-S. Jao and A. M. Shkel, "Directional ranging for enhanced performance of aided pedestrian inertial navigation," in *IEEE International Symposium on Inertial Sensors and Systems (INERTIAL)*, Naples, 2019.

[10] J. Rantanen, L. Ruotsalainen, M. Kirkko-Jaakkola and M. Mäkelä, "Height measurement in seamless indoor/outdoor infrastructure-free navigation," *IEEE Transactions on Instrumentation and Measurement,* vol. 68, pp. 1199-1209, 2018.

[11] J.-O. Nilsson, I. Skog and P. Händel, "A note on the limitations of ZUPTs and the implications on sensor error modeling," in *International Conference on Indoor Positioning and Indoor Navigation (IPIN)*, Sydney, 2012.

[12] K. D. Rao, "Integration of GPS and baro-inertial loop aided strapdown INS and radar altimeter," *IETE Journal of Research,* vol. 43, pp. 383-390, 1997.

[13] Y. Jiong, Z. Lei, D. Jiangping, S. Rong and W. Jianyu, "GPS/SINS/BARO integrated navigation system for UAV," in *IEEE International Forum on Information Technology and Applications (IFITA)*, Kunming, 2010.

[14] V. S. Sokolovic, G. Dikic and R. Stancic, "Integration of INS, GPS, magnetometer and barometer for improving accuracy navigation of the vehicle," *Defense Science Journal,* vol. 63, pp. 451-455, 2013.

[15] J. Zhang, E. Edwan, J. Zhou, W. Chai and O. Loffeld, "Performance investigation of barometer aided GPS/MEMS-IMU integration," in *IEEE/ION Position, Location and Navigation Symposium,* Myrtle Beach, South Carolina, USA, 2012.

[16] A. Sabatini and V. Genovese, "A sensor fusion method for tracking vertical velocity and height based on inertial and barometric altimeter measurements," *Sensors,* vol. 14, pp. 13324-13347, 2014.

[17] Z. Xinxi, Z. Rong, G. Meifeng, C. Gaofeng, N. Shulai and L. Jinglong, "The performance impact evaluation on bias of gyro and accelerometer for foot-mounted INS," in *IEEE International Conference on Electronic Measurement & Instruments (ICEMI)*, Qingdao, 2015.

[18] C.-S. Jao, Y. Wang, S. Askari and A. M. Shkel, "A Closed-Form Analytical Estimation of VerticalDisplacement Error in Pedestrian Navigation," in *IEEE/ION Position, Location and Navigation Symposium*, Portland, 2020.

[19] F. Le Blancq, "Diurnal pressure variation: the atmospheric tide," *Weather,* vol. 66, pp. 306-307, 2011.

[20] J. Käppi and K. Alanen, "Pressure altitude enhanced AGNSS hybrid receiver for a mobile terminal," in *ION GPS*, Long Beach, CA, USA, 2005.

[21] G. Retscher, "Altitude determination of a pedestrian in a multistorey building," in *Location based services and telecartography*, Springer, 2007, pp. 119-130.

[22] M. Tanigawa, H. Luinge, L. Schipper and P. Slycke, "Drift-free dynamic height sensor using MEMS IMU aided by MEMS pressure sensor," in *5th Workshop on Positioning, Navigation and Communication*, Hannover, 2008.

[23] J. Parviainen, J. Kantola and J. Collin, "Differential barometry in personal navigation," in *IEEE/ION Position, Location and Navigation Symposium*, Monterey, 2008.

[24] H. Xia, X. Wang, Y. Qiao, J. Jian and Y. Chang, "Using multiple barometers to detect the floor location of smart phones with built-in barometric sensors for indoor positioning," *Sensors,* vol. 15, pp. 7857-7877, 2015.

[25] J. Rantakokko, J. Rydell, P. Strömbäck, P. Händel, J. Callmer, D. Törnqvist, F. Gustafsson, M. Jobs and M. Grudén, "Accurate and reliable soldier and first responder indoor positioning: multisensor systems and cooperative localization," *IEEE Wireless Communications*, vol. 18, pp. 10-18, 2011.

[26] U. Walder and T. Bernoulli, "Context-adaptive algorithms to improve indoor positioning with inertial sensors," in *International Conference on Indoor Positioning and Indoor Navigation (IPIN),* Zurich, 2010.

[27] G. Xu, T. Meng and H. Zhang, "Height Estimation of Ultrasonic Array Based on Integrated Navigation for UAVs," in *Chinese Control And Decision Conference (CCDC),* Nanchang, 2019.

[28] K. Gadek and M. Jaraczewski, "Novel ultrasonic distance measuring system based on correlation method," *MEASUREMENT SCIENCE REVIEW,* vol. 14, p. 331–336, 2014.

[29] L. Koval, J. Vaňuš and P. Bilík, "Distance measuring by ultrasonic sensor," *IFAC-PapersOnLine,* vol. 49, pp. 153-158, 2016.

[30] P. D. Duong and Y. S. Suh, "Foot pose estimation using an inertial sensor unit and two distance sensors," *Sensors,* vol. 15, pp. 15888-15902, 2015.

[31] S. Askari, C.-S. Jao, Y. Wang and A. M. Shkel, "A Laboratory Testbed for Self-Contained Navigation," in *IEEE International Symposium on Inertial Sensors and Systems (INERTIAL)*, Naples, 2019.

[32] A. R. Jiménez, F. Seco, F. Zampella, J. C. Prieto and J. Guevara, "PDR with a foot-mounted IMU and ramp detection," *Sensors*, vol. 11, pp. 9393-9410, 2011.

[33] I. Skog, P. Handel, J.-O. Nilsson and J. Rantakokko, "Zero-velocity detection—An algorithm evaluation," *IEEE transactions on biomedical engineering*, vol. 57, pp. 2657-2666, 2010.

[34] T. Yang, K. Kaji and N. Kawaguchi, "Elevator acceleration sensing: Design and estimation recognition algorithm using crowdsourcing," in *IEEE 37th Annual Computer Software and Applications Conference Workshops (COMPSACW)*, Kyoto, 2013.